Nonlinear Dynamics and Systems Theory, **9** (3) (2009) 287–299

Robust Controller Design for Active Flutter Suppression of a Two-dimensional Airfoil

Chunyan Gao*, Guangren Duan and Canghua Jiang

Center for Control Theory and Guidance Technology, Harbin Institute of Technology, P.O.Box 416, Harbin 150001, PRC

Received: June 11, 2008; Revised: June 8, 2009

Abstract: This paper investigates the problem of active flutter suppression for a two-dimensional three degrees of freedom (3DOF) airfoil. With the influence of unsteady aerodynamic forces and parametric uncertainties, the output suboptimal control law design for a 3DOF airfoil control system is transformed into a constrained optimization problem. Then, the flutter robust suppression control law could be expediently obtained by linear matrix inequalities (LMIs), which realizes active flutter suppression by increasing the flutter critical speed. Simulation results show that the flutter phenomenon could be well suppressed in spite of the uncertainty of damping coefficients.

Keywords: *active flutter suppression; suboptimal control; linear matrix inequalities.*

Mathematics Subject Classification (2000): 93C95, 93B12, 93D21.

1 Introduction

Recently, techniques of active aeroelastic wing [8], thrust vector control [1, 4] and flying-wing layout [2, 4] have became the hottest issues in aeronautic area. At the same time, high-altitude long-endurance aircrafts are taken into account by more and more countries [7]. The general features of high-altitude long-endurance aircraft are high aspect ratio, light structural weight, and well flexibility. Therefore, the future aircrafts are in the nature of more flexibility. With the increase of flexibility, the flutter phenomenon is more and more prominent. Flutter is a vibration caused by airstream energy being absorbed by the lifting surface, which is more likely to occur in the wings, ailerons and other flexible parts. Furthermore, this aeroelastic phenomenon increasing with the flight velocities can cause the wing fatigue to be increased. If the flight velocity is above the critical flutter

* Corresponding author: chygao@yahoo.com.cn

speed and the flutter phenomenon is not suppressed, the structure of aircrafts may be destroyed. To reduce or suppress this phenomenon is very important in the aeronautic industry.

Over the past several decades, this severe problem has been studied using many different techniques. Traditional technique is the passive flutter suppression method, which adds structural weight to change the aircraft stiffness, and some components have to be moved to keep balance. So this technique deteriorates some flight performances, and is not always feasible. Later the active flutter suppression method appears to suppresses flutter phenomenon without adding structural weight and redesign. The idea of this method is to introduce a certain deformation based on the structure flexibility, which can suppress the flutter actively. Therefore, there are above two main techniques that we can use.

With the development of active control technology in the aeronautic area, flexibility at the support of active control technology exhibits more potential. Nowadays, more and more active control techniques are used to suppress the flutter phenomenon. Shana D. Olds uses Linear Quadratic Regulation theory to design a state feedback controller for an aeroelastic system [6]. Good performances are illustrated, but the results are not feasible in practice because all states are assumed to be measurable. Samuel da Silva and Vicente L. Júnior used the LMI technique to solve the active flutter suppression problem with robustness to polytopic parametric uncertainties [9]. In their paper, they designed a state feedback control law based on full-order state observer. The dimension of state observer is equal to that of controlled plant. Therefore, there are twenty-order states in their closed-loop aeroelastic system. Though the state feed back control law and observer can be designed respectively according to separate principle, the full-order observer is difficult to carry out in actual engineering application because of high order. In the view of engineering practice, convenient and effective design process play an important role in actual aeroelastic system, which motivates us to carry out the present study.

In this paper, for the sake of analysis, the model is simplified on the assumption that the stiffness of control surface is very large, which is different from the aeroelastic model of aforementioned papers [6, 9]. We adopt the output as the feedback information to design a robust controller for active flutter suppression of a two-dimensional 3DOF airfoil aeroelastic system. Considering the system with polytopic parametric uncertainties and the influence of unsteady aerodynamic forces, we transform the output suboptimal control law design for a 3DOF airfoil control system into a constrained optimization problem, then obtain the output feedback control law by LMI technique and the minimum norm method. Despite the uncertainties of two-dimensional 3DOF airfoil aeroelastic system, this proposed approach makes it design easier for engineering application. In addition, it considers both response performance and control performance. This approach can conveniently and effectively realize robust active flutter suppression. The simulation results show that the flutter phenomenon could be well suppressed in spite of the uncertainty of damping coefficients.

2 Aeroelastic System Formulation

The schematic diagram of a 3DOF airfoil aeroelastic system with control surface is shown in Figure 2.1. Here, in order to develop the motion equations a coordinate system is introduced, which originates at the midpoint of airfoil chord. The x axis lies along the chord in the horizontal direction. The z axis shown in Figure 2.1 is perpendicular with x

direction. The quantity b is half chord. And two springs, one of which is line spring, the other is torsional spring, are put on the point E of airfoil elastic axis which is located at a distance of ab from the mid-chord. The flap hinge is located at a distance of cb from the mid-chord. Then, the three degrees of freedom are respectively the plunge h which is measured at the elastic axis E and positive in the downward direction, the pitching angle α which rotates on the elastic axis E and positive nose-up, the deflective angle of control surface β which represents the angular deflection of the flap about the flap hinge and positive for the flap trailing edge down.

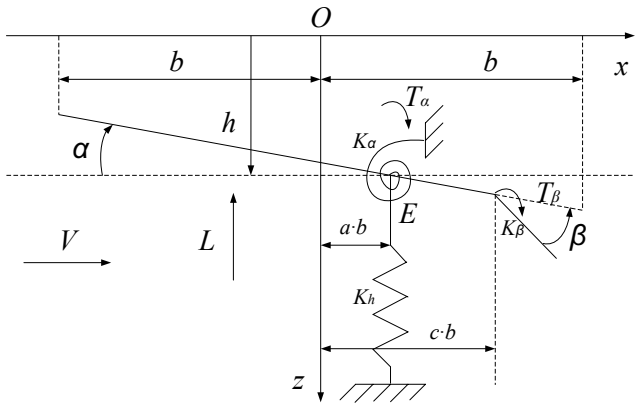

Figure 2.1: Configuration of a two-dimensional 3DOF airfoil.

2.1 Unsteady aerodynamic force calculation

The precise calculation of unsteady aerodynamic forces is an important step in two-dimensional airfoil flutter analysis. According to the Theodorsen theory, the aerodynamic lift L, pitching moment T_α, and control surface moment T_β of a unit wingspan length are respectively:

$$
\begin{aligned}
L &= \pi\rho b^2\left(\ddot{h}+V\dot{\alpha}-ba\ddot{\alpha}-\frac{V}{\pi}T_1\dot{\beta}-\frac{b}{\pi}T_4\ddot{\beta}\right)+2\pi\rho VbT_0C\left(k\right),\\
T_\alpha &= \pi\rho b^2\left[ba\ddot{h}-Vb\left(\frac{1}{2}-a\right)\dot{\alpha}-b^2\left(\frac{1}{8}+a^2\right)\ddot{\alpha}-\frac{V^2}{\pi}\left(T_4+T_{10}\right)\beta+\right.\\
&\quad \left.\frac{Vb}{\pi}\left(-T_1+T_8+\left(c-a\right)T_4-\frac{1}{2}T_{11}\right)\dot{\beta}+\frac{b^2}{\pi}\left(T_7+\left(c-a\right)T_1\ddot{\beta}\right)\right]\\
&\quad +2\pi\rho Vb^2\left(\bar{a}+\frac{1}{2}\right)T_0C\left(k\right),\\
T_\beta &= \pi\rho b^2\left[\frac{b}{\pi}T_1\ddot{h}-\frac{Vb}{\pi}\left(2T_9+T_1-\left(a-\frac{1}{2}\right)T_4\right)\dot{\alpha}-\frac{2b^2}{\pi}T_{13}\ddot{\alpha}\right.\\
&\quad \left.-\left(\frac{V}{\pi}\right)^2\left(T_5-T_4T_{10}\right)\beta+\frac{Vb}{2\pi^2}T_4T_{11}\dot{\beta}+\left(\frac{b}{\pi}\right)^2T_3\ddot{\beta}\right]-\rho Vb^2T_{12}T_0C\left(k\right).
\end{aligned}
$$

where k is the air reduced frequency which is dimensionless, ρ is the air density, and V is the flow velocity. Definitions of other coefficients could be found in [10].

2.2 Aeroelastic System Modeling

In the dynamic schematic diagram Figure 2.1, any point displacement of the airfoil can be expressed as

$$z = h + (x - ab)\,\alpha + (x - cb)\,\beta U_{\text{step}}\,(x - cb)\,,$$

where $U_{\text{step}}\,(x - cb)$ is an unit step function.

Then, the system kinetic energy is

$$\begin{aligned} T &= \frac{1}{2}\int_{-b}^{b} \dot{z}^2 \bar{m} dx \\ &= \frac{1}{2} m\dot{h}^2 + \frac{1}{2} I_\alpha \dot{\alpha}^2 + \frac{1}{2} I_\beta \dot{\beta}^2 + S_\alpha \dot{h}\dot{\alpha} + S_\beta \dot{h}\dot{\beta} + \left[(c-a)\,bS_\beta + I_\beta\right]\dot{\alpha}\dot{\beta}, \end{aligned}$$

and the potential energy is

$$U = \frac{1}{2} k_h h^2 + \frac{1}{2} k_\alpha \alpha^2 + \frac{1}{2} k_\beta \beta^2,$$

where

$$\begin{aligned} m &= \int_{-b}^{b} \bar{m} dx, \\ S_\alpha &= \int_{-b}^{b} (x - ab)\,\bar{m} dx = m x_a, \\ I_\alpha &= \int_{-b}^{b} (x - ab)^2\,\bar{m} dx = m r_a^2, \\ S_\beta &= \int_{cb}^{b} (x - cb)\,\bar{m} dx = m x_\beta, \\ I_\beta &= \int_{cb}^{b} (x - cb)^2\,\bar{m} dx = m r_\beta^2, \end{aligned}$$

k_h, k_α, k_β are stiffness coefficients, $\bar{m}$ is airfoil mass of unit area. Definitions of other coefficients could be found in [11].

According to Lagrange's equation and principle of virtual work, the equation of motion for this two-dimensional 3DOF airfoil aeroelastic system is

$$\begin{bmatrix} m & m x_\alpha & m x_\beta \\ m x_\alpha & m r_\alpha^2 & m r_\beta^2 + m x_\beta (cb - ab) \\ m x_\beta & m r_\beta^2 + m x_\beta (cb - ab) & m r_\beta^2 \end{bmatrix} \begin{bmatrix} \ddot{h} \\ \ddot{\alpha} \\ \ddot{\beta} \end{bmatrix}$$

$$+ \begin{bmatrix} d_h & 0 & 0 \\ 0 & d_\alpha & 0 \\ 0 & 0 & d_\beta \end{bmatrix} \begin{bmatrix} \dot{h} \\ \dot{\alpha} \\ \dot{\beta} \end{bmatrix} + \begin{bmatrix} k_h & 0 & 0 \\ 0 & k_\alpha & 0 \\ 0 & 0 & k_\beta \end{bmatrix} \begin{bmatrix} h \\ \alpha \\ \beta \end{bmatrix} = \begin{bmatrix} -L \\ T_\alpha \\ T_\beta \end{bmatrix}$$

On the assumption of perfect rigidity, i.e. the stiffness of control surface is very large, after introducing some damping coefficients, and the unsteady aerodynamic forces, the open-loop motion model of a 3DOF airfoil can be represented as [11]

$$\left(s^2 \left[\begin{array}{cc} M_s & M_c \end{array}\right] + s \left[\begin{array}{cc} D_s & 0 \end{array}\right] + \left[\begin{array}{cc} K_s & 0 \end{array}\right]\right) \left[\begin{array}{c} q_s(s) \\ \beta(s) \end{array}\right]$$

$$+q_d \left[\begin{array}{cc} \tilde{A}_s(s) & \tilde{A}_c(s) \end{array}\right] \left[\begin{array}{c} q_s(s) \\ \beta(s) \end{array}\right] = 0 \tag{2.1}$$

where $q_s = \left[\begin{array}{cc} h & \alpha \end{array}\right]^T$, M_s, D_s, K_s are respectively the mass matrix, structural damping matrix, and structural stiffness matrix of plunge and pitching modes, M_c is the coupled mass matrix among the control surface and structural modes, $\tilde{A}_s(s)$ and $\tilde{A}_c(s)$ are the matrices of aerodynamic forces, $q_d = \frac{1}{2}\rho V^2$ is the dynamic pressure of a gas flow.

For the sake of convenience, Eq. (2.1) could be rearranged into the following form:

$$\left(M_s s^2 + D_s s + K_s\right) q_s(s) + M_c s^2 \beta(s) + q_d \tilde{A}_s(s) q_s(s) + q_d \tilde{A}_c(s) \beta(s) = 0.$$

In order to obtain a state space representation, a rational function approximation, that is, the minimum states method, is adopted to fix the unsteady aerodynamic matrices in frequency domain to the matrices in Laplace domain. Therefore we have

$$\tilde{A}_s(s) = A_{s0} + \frac{b}{V} A_{s1} s + \frac{b^2}{V^2} A_{s2} s^2 + E\left(Is - \frac{V}{b} R\right)^{-1} F_s s, \tag{2.2}$$

$$\tilde{A}_c(s) = A_{c0} + \frac{b}{V} A_{c1} s + \frac{b^2}{V^2} A_{c2} s^2 + E\left(Is - \frac{V}{b} R\right)^{-1} F_c s. \tag{2.3}$$

And aerodynamic augmented states

$$x_a(s) = \left(Is - \frac{V}{b} R\right)^{-1} \left(F_s q_s(s) + F_c \beta(s)\right) s \tag{2.4}$$

are introduced.

According to formula (2.2), (2.3) and (2.4), Eq. (2.1) can be rewritten into the state space form:

$$\dot{X}_h = A_h X_h + B_h u_h,$$

where

$$X_h = \left[\begin{array}{c} q_s \\ \dot{q}_s \\ x_a \end{array}\right], \; u_h = \left[\begin{array}{c} \beta \\ \dot{\beta} \\ \ddot{\beta} \end{array}\right],$$

$$\begin{aligned} A_h &= \left[\begin{array}{ccc} 0 & I & 0 \\ -M^{-1}\left(K_s + q_d A_{s0}\right) & -M^{-1}\left(D_s + q_d \frac{b}{V} A_{s1}\right) & -q_d M^{-1} E \\ 0 & F_s & \frac{V}{b} R \end{array}\right], \\ B_h &= \left[\begin{array}{ccc} 0 & 0 & 0 \\ -q_d M^{-1} A_{c0} & -q_d \frac{b}{V} M^{-1} A_{c1} & -M^{-1}\left(M_c + q_d \frac{b^2}{V^2} A_{c2}\right) \\ 0 & F_c & 0 \end{array}\right], \\ M &= M_s + q_d \frac{b^2}{V^2} A_{s2}. \end{aligned}$$

In practice, information of displacement, velocity, and acceleration can be obtained by sensors, such as accelerometers and angular rate gyros. It is assumed that in this two dimensional 3DOF aeroelastic system the acceleration information can be measured by gyros which takes the following form [11]

$$\begin{aligned} Y_h &= \Phi \left[\begin{array}{ccc} -M^{-1}\left(K_s + q_d A_{s0}\right) & -M^{-1}\left(D_s + q_d \frac{b}{V} A_{s1}\right) & -q_d M^{-1} E \end{array} \right] \left[\begin{array}{c} q \\ \dot{q} \\ x_a \end{array} \right] \\ &\quad + \Phi \left[\begin{array}{ccc} -q_d M^{-1} A_{c0} & -q_d \frac{b}{V} M^{-1} A_{c1} & -M^{-1}\left(M_c + q_d \frac{b^2}{V^2} A_{c2}\right) \end{array} \right] \left[\begin{array}{c} \beta \\ \dot{\beta} \\ \ddot{\beta} \end{array} \right], \end{aligned}$$

where Φ is the coefficient matrix. Then the output state function of the two-dimensional 3DOF aeroelastic system could be denoted as

$$Y_h = C_h X_h + D_h u_h.$$

Furthermore, we adopt the following transfer function to describe the relation between the deflective angle of control surface and the command of actuator

$$\frac{\beta}{\delta_c} = \frac{a_3}{s^3 + a_2 s^2 + a_1 s + a_0},$$

which has the following representation in time domain

$$\left[\begin{array}{c} \dot{\beta} \\ \ddot{\beta} \\ \dddot{\beta} \end{array} \right] = \left[\begin{array}{ccc} 0 & 1 & 0 \\ 0 & 0 & 1 \\ -a_0 & -a_1 & -a_2 \end{array} \right] \left[\begin{array}{c} \beta \\ \dot{\beta} \\ \ddot{\beta} \end{array} \right] + \left[\begin{array}{c} 0 \\ 0 \\ a_3 \end{array} \right] \delta_c.$$

Then, the final open-loop aeroelastic state and output functions are

$$\begin{aligned} \dot{X} &= AX + Bu, \\ Y &= CX, \end{aligned}$$

where

$$X = \left[\begin{array}{cc} X_h & X_e \end{array} \right]^T,\ u = \delta_c,\ X_e = \left[\begin{array}{ccc} \beta & \dot{\beta} & \ddot{\beta} \end{array} \right]^T,$$

$$A = \left[\begin{array}{cc} A_h & B_h \\ 0 & A_e \end{array} \right],\ B = \left[\begin{array}{c} 0 \\ B_e \end{array} \right],\ C = \left[\begin{array}{cc} C_h & D_h \end{array} \right],$$

$$A_e = \left[\begin{array}{ccc} 0 & 1 & 0 \\ 0 & 0 & 1 \\ -a_0 & -a_1 & -a_2 \end{array} \right],\ B_e = \left[\begin{array}{c} 0 \\ 0 \\ a_3 \end{array} \right].$$

Since matrix A depends on the flow velocity V explicitly, in the following matrix A is substituted by $A(V)$. It is clear that eigenvalues of $A(V)$ change their positions on complex plan with V. According to the linear control theories, the system is stable if and only if the eigenvalues of state matrix are located in the open left-half complex plane. Therefore, when the locus of a eigenvalue crosses the imaginary axis from the left-half complex plane, the aeroelastic system is critically stable. And the corresponding flow velocity is called a critical flutter speed.

3 Robust Control Law Design for Active Flutter Suppression

3.1 Problem Formulation

In the aeroelastic control systems, the most common technique for active flutter suppression is the theory of Linear Quadratic Regulation by state feedback. Since the aerodynamic augmented states are immeasurable, this technique has difficulties to be applied in practice. Therefore, output feedback is adopted in this paper.

According to the two-dimensional 3DOF aeroelastic system model

$$\begin{aligned} \dot{X} &= A(V)X + Bu, \\ Y &= CX, \end{aligned} \tag{3.1}$$

and supposing that the matrix C is of full row rank, we design the following output feedback control law

$$u = -KY \tag{3.2}$$

to minimize the cost function

$$J = \frac{1}{2}\int_0^\infty \left(X^T Q X + u^T R u\right) dt. \tag{3.3}$$

Generally the weighting matrices Q and R are selected via engineering experiences. In this paper, the two weighting matrices are both assumed to be positive definite. Q is limited to 10^{-3} level, and R is limited to an identity matrix.

Usually there are three approaches, i.e. the Levine-Athans method, the least error excitation method, and the minimum norm method [13], to solve the output suboptimal problem and obtain the output feedback control law K indirectly. But the actual two-dimensional 3DOF system works in a changing environment, which differs from the model that we discuss and design, especially when the damping coefficients are difficult to be obtained precisely. Therefore the model we analysis possesses uncertainties. In this paper, we assume that the dynamic matrix has a parametric uncertainty which can be described by a polytope, i.e.

$$A \in \Omega = Co\{A_1, A_2, \cdots, A_n\} = \left\{ \sum_{i=1}^{n} \lambda_i A_i; \lambda_i \geq 0, \sum_{i=1}^{n} \lambda_i = 1 \right\},$$

where n is the number of vertexes of the polytopic system. In addition, the formula $q_d = \frac{1}{2}\rho V^2$ is included in every matrix A_i. Therefore, the matrix A_i also depends on the flow velocity V.

3.2 Robust Control Law Design

The problem to be investigated in this paper is how to design the output feedback control law (3.2). With the control law, the two-dimensional 3DOF aeroelastic system (3.1) can be represented as:

$$\dot{X} = (A - BKC)X, \ A \in \Omega.$$

Then, the cost function could be rewritten into the following form:

$$J = \frac{1}{2}\int_0^\infty X^T \left(Q + C^T K^T R K C\right) X dt.$$

The system described by (3.1) is quadratically stable if and only if there exists a symmetric matrix $P = P^T > 0$ such that

$$(A - BKC)^T P + P(A - BKC) + Q + C^T K^T RKC \leq 0. \tag{3.4}$$

Along any trajectory of the closed-loop system, the derivative of $X^T(t) PX(t)$ is

$$\begin{aligned} \frac{d}{dt}\left[X^T(t) PX(t)\right] &= X^T(t)\left[(A - BKC)^T P + P(A - BKC)\right] X(t) \\ &\leq -X^T(t)\left(Q + C^T K^T RKC\right) X(t). \end{aligned} \tag{3.5}$$

After integrating both sides of the inequality (3.5) from $t = 0$ to $t = \infty$, we have

$$J = \frac{1}{2}\int_0^\infty X^T\left(Q + C^T K^T RKC\right) X dt \leq X^T(0) PX(0).$$

Therefore the suboptimal control problem could be transformed into a constrained optimization problem

$$\begin{aligned} &\min \frac{1}{2} X^T(0) PX(0) \\ &\text{s.t.} \begin{cases} (A - BKC)^T P + P(A - BKC) + Q + C^T K^T RKC \leq 0, \\ P > 0,\ Q > 0,\ R > 0. \end{cases} \end{aligned} \tag{3.6}$$

It is noted that since our purpose is to determine the matrix K, inequality (3.4) is actually a nonlinear matrix inequality. This drawback can be overcome by defining $P_1 = P^{-1}$, $P_2 = -KCP_1$, and inequality (3.4) is equivalent to the following LMI

$$\begin{bmatrix} P_1 A^T + AP_1 + P_2^T B^T + BP_2 & P_1 & P_2^T \\ P_1 & -Q^{-1} & 0 \\ P_2 & 0 & -R^{-1} \end{bmatrix} \leq 0.$$

Obviously, when the dynamic matrix A has a polytopic parametric variation, we only need analyze this problem on the vertexes [3, 5, 12]. Thus, the optimization problem (3.6) could be transformed further into the following form:

$$\begin{aligned} &\min\ \gamma \\ &\text{s.t.} \begin{cases} \begin{bmatrix} P_1 A_i^T + A_i P_1 + P_2^T B^T + BP_2 & P_1 & P_2^T \\ P_1 & -Q^{-1} & 0 \\ P_2 & 0 & -R^{-1} \end{bmatrix} \leq 0, \\ \begin{bmatrix} \gamma & X^T(0) \\ X(0) & P_1 \end{bmatrix} \geq 0, \\ P_1 > 0, \end{cases} \end{aligned} \tag{3.7}$$

where $P_1 = P^{-1}$, $P_2 = -KCP_1$, $i = 1, 2, \cdots n$.

Because the output matrix C is not always square, we could not directly inverse CP_1 to derive K from equation $P_2 = -KCP_1$. In this paper, we apply the minimum norm method to determine the matrix K indirectly. Define $F^* \triangleq -P_2 P_1^{-1}$, $F \triangleq KC$. Supposing that the matrices P_1 and P_2 have been derived from the optimization problem (3.7), minimizing the following objective function

$$J = \| F - F^* \| = \sqrt{\mathrm{Trace}\,(F - F^*)^T (F - F^*)},$$

we can get the approximate solution

$$K = F^* C^T \left(CC^T\right)^{-1}.$$

4 Numerical Simulation

4.1 Open-loop Simulation

In order to validate the effectiveness of the proposed method, numerical simulation are set up in this section with the following parameters. Here parameter variations are not

Parameter	Value	Parameter	Value
m	1.285kg	S_α	0.0209kgm
S_β	0.0006608kgm	I_α	0.005142kgm^2
a	-0.5	b	0.1m
c	0.5	ρ	1.025kg/m^3
k_h	2742N/m	k_α	2.912Nm/rad
k_β	90042Nm/rad	d_h	30.43Ns/m
d_α	0.04Ns/m	d_β	418.8977Ns/m

Table 4.1: List parameters.

considered. Under the influence of the unsteady aerodynamic forces, the root locus of the open loop aeroelastic system are showed in Figure 4.1. And the real parts of the eigenvalues of $A(V)$ with respect to the flow velocities are showed in Figure 4.2. If the real parts of all of the eigenvalues of $A(V)$ are negative, that is, the eigenvalues are in the open left half plane, the two-dimensional 3DOF aeroelastic system is asymptotically stable. From Figure 4.1 and Figure 4.2 we can see that the pitching mode will be in the right half plane when the flow velocity exceeds 47.5m/s, and then flutter occurs. The flutter speed, $V_f = 47.5$m/s, is the speed at which the open loop system becomes marginally stable.

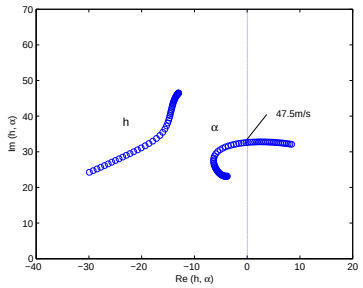

Figure 4.1: The root locus of the open loop aeroelastic system.

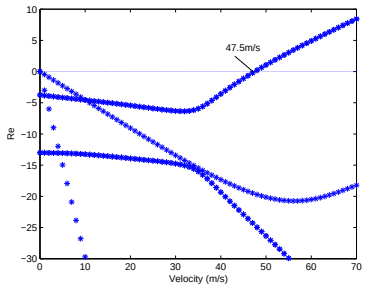

Figure 4.2: The relation between real parts of eigenvalues and flow velocity.

Here we select three velocity values to see the time response of each modes without considering uncertainties in any parameter. From Figures 4.3, 4.4 and 4.5 we could see the plunge, pitching and control surface states are asymptotically stable at $V = 46$m/s,

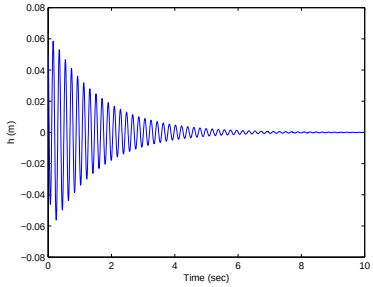

Figure 4.3: The time response curve of plunge mode at V=46m/s.

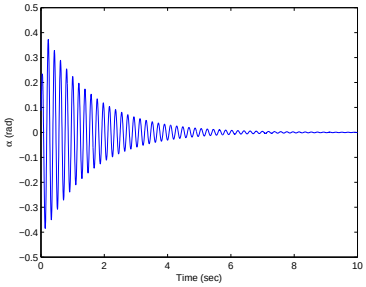

Figure 4.4: The time response curve of pitching mode at V=46m/s.

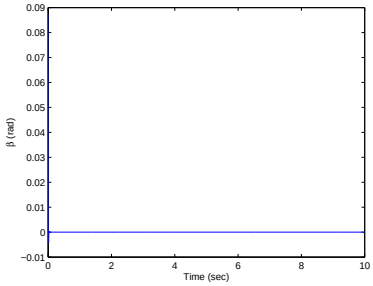

Figure 4.5: The time response curve of control surface mode at V=46m/s.

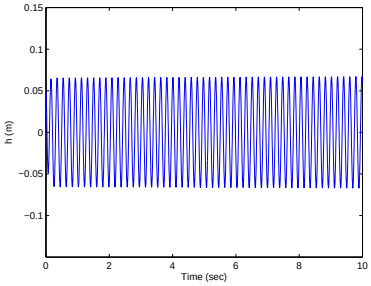

Figure 4.6: The time response curve of plunge mode at V=47.5m/s.

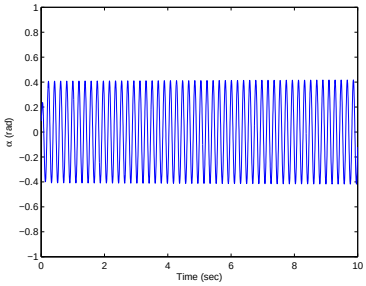

Figure 4.7: The time response curve of pitching mode at V=47.5m/s.

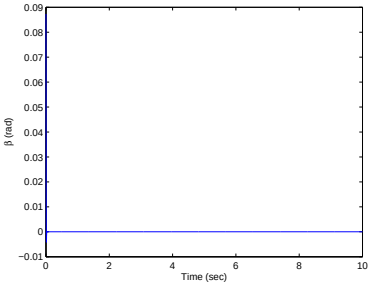

Figure 4.8: The time response curve of control surface mode at V=47.5m/s.

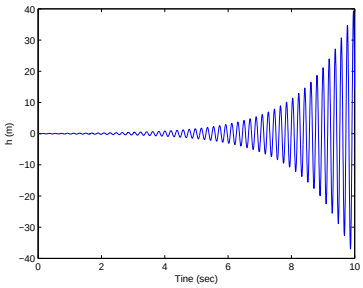

Figure 4.9: The time response curve of plunge mode at V=49m/s.

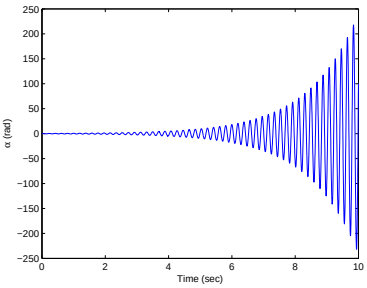

Figure 4.10: The time response curve of pitching mode at V=49m/s.

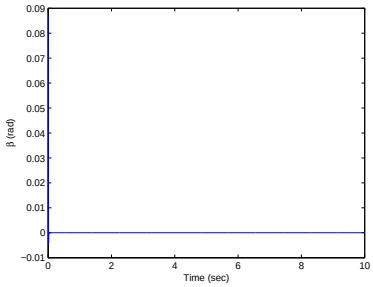

Figure 4.11: The time response curve of control surface mode at V=49m/s.

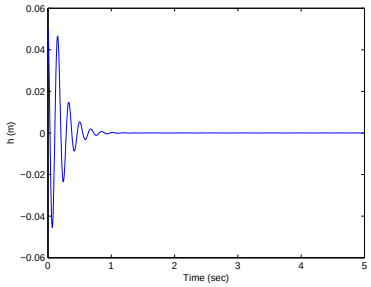

Figure 4.12: The time response curve of plunge mode at V=49m/s after robust flutter suppression.

and almost all oscillations disappear at $t = 7$ seconds. So, the flutter phenomenon could be suppressed by the aeroelastic system itself. At $V = V_f = 47.5$m/s, the sates are all settled into harmonic oscillations as shown in Figures 4.6, 4.7, 4.8. But in Figures 4.9, 4.10, and 4.11, with flow velocity $V = 49$m/s, the plunge, pitching and control surface states continue to increase without bound, and after about 6 seconds, the oscillations are so severe that the airfoil would become unstable. Furthermore, from Figure 4.11 we could see that the state of control surface β is always stable even though the flow velocity exceeds the critical flutter speed, which coincides with the assumption of the perfect rigid control surface.

In brief, for $V < V_f$ the system is asymptotically stable. And for $V > V_f$ the system is unable, in this case wing separation will occur which is dangerous for a real aircraft.

4.2 Closed-loop Simulation

In this section a robust controller is designed for the two-dimensional 3DOF airfoil aeroelastic system using the proposed method. Because the damping coefficients are difficult to be obtained precisely, the damping coefficients are assumed to be uncertain which have possible variations of $\pm 10\%$ around the nominal values. The robust output feedback gain matrix is obtained by $K = F^* C^T \left(CC^T\right)^{-1}$, where F^* is the solution to the optimization problem (3.7).

Figures 4.12, 4.13, and 4.14 illustrate the time response curves at $V = 49$m/s, from which we can see the flutter phenomenon is well suppressed after about 1 second and the output feedback is robust to the considered parametric variations.

Furthermore, we are interested in the performance when the flow velocity exceeds the critical flutter speed and the control is delayed by a few seconds. We investigate the system response with parametric uncertainties when the control is initiated at a time greater than $t = 0$ seconds. Consequently, with flow velocity 49m/s, and the control initiated at 2 seconds. the time responses are shown in Figures 4.15, 4.16, 4.17. The oscillation disappear at $t = 3$ seconds and the output feedback is robust to the considered parametric variations as well.

The relation between the real parts of $A(V)$ eigenvalues and the flow velocity with flutter robust suppression is shown in Figure 4.18, from which we could see the critical flutter speed is 57.8m/s, that is, the critical speed increase from the original speed 47.5m/s to 57.8m/s. The critical flutter speed increases 21.68%. From the simulations

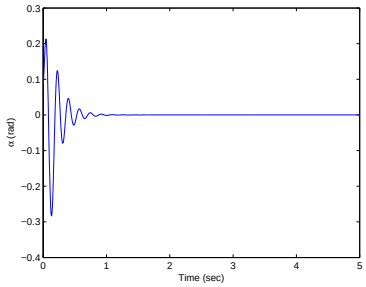

Figure 4.13: The time response curve of pitching mode at V=49m/s after robust flutter suppression.

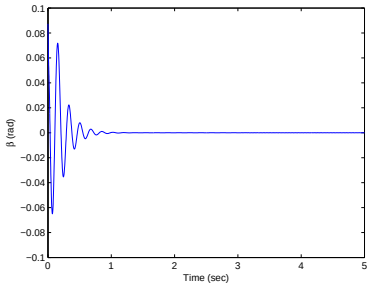

Figure 4.14: The time response curve of control surface mode at V=49m/s after robust flutter suppression.

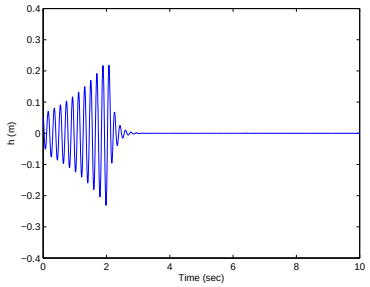

Figure 4.15: The time response curve of plunge mode at V=49m/s after robust flutter suppression: t=2 seconds.

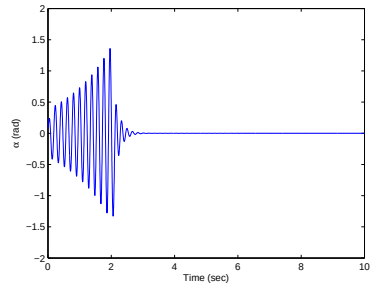

Figure 4.16: The time response curve of pitching mode at V=49m/s after robust flutter suppression: t=2 seconds.

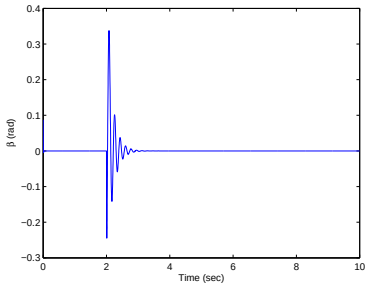

Figure 4.17: The time response curve of control surface mode at V=49m/s after robust flutter suppression: t=2 seconds.

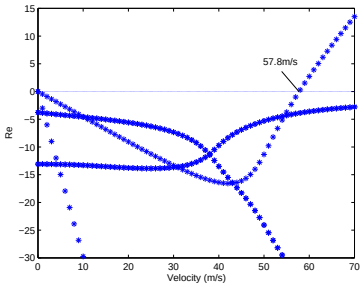

Figure 4.18: The relation between real parts of eigenvalues and flow velocity after robust flutter suppression.

we can conclude that the proposed method not only well suppresses flutter phenomenon, but also increases the critical flutter speed.

5 Conclusion

In the traditional aircraft design, a passive method is usually adopted, which increases the structure weight of the aircraft in order to increase the critical flutter speed. In this paper we present an active control approach, which transforms the suboptimal control law design problem into a constrained optimization problem, to design the robust control law of a two-dimensional 3DOF aeroelastic system. The introduced deformation can suppress the flutter phenomenon by the flexibility of structure. The simulation results show that the minimum norm method and the LMI technique adopted is valid with the uncertainties of damping coefficients. When the flow velocity exceeds the critical flutter speed, the two-dimensional 3DOF airfoil is still stable with the proposed robust controller.

References

[1] Atesoglu, Ö. and Özgören, M. High-Flight Maneuverability Enhancement of a Fighter Aircraft Using Thrust-Vectoring Control. *Journal of Guidance, Control and Dynamics* **30**(5) (2007) 1480–1493.

[2] Bolsunovsky, A., Buzoverya, N., Gurevich, B., Denisov, V., Dunaevsky, A., Shkadov, L., Sonin, O., Udzhuhu, A. and Zhurihin, J. Flying wing-problems and decisions. *Aircraft Design* **4**(4) (2001) 193–219.

[3] Boyd, S. and Vandenberghe, L. *Convex Optimization*. Cambridge University Press, Cambridge, 2004.

[4] Jadbabaie, A. and Hauser, J. Control of a thrust-vectored flying wing: a receding horizon-LPV approach. *International Journal of Robust and Nonlinear Control* **12**(9) (2002) 869–896.

[5] Karimi, H., Lohmann, B. and Buskens, C. An LMI Approach to H_∞ Filtering for Linear Parameter-Varying Systems with Delayed States and Outputs. *Nonlinear Dynamics and Systems Theory* **7**(4) (2006) 351–368.

[6] Olds, S. *Modeling and LQR Control of a Two-Dimensional Airfoil*. PhD thesis, Virginia Polytechnic Institute and State University, 1997.

[7] Patil, M., Hodges, D. and Cesnik, C. Nonlinear aeroelasticity and flight dynamics of high-altitude long-endurance aircraft. *Journal of Aircraft* **38**(1) (2001) 88–94.

[8] Pendleton, E., Bessette, D., Field, P., Miller, G. and Griffin, K. Active Aeroelastic Wing Flight Research Program: Technical Program and Model Analytical Development. *Journal of Aircraft* **37**(4) (2000) 554–561.

[9] Silva, S. and V. Lopes Júnior. Active flutter suppression in a 2-D airfoil using linear matrix inequalities techniques. *Journal of the Brazilian Society of Mechanical Sciences and Engineering* **28** (2006) 84–93.

[10] Theodorsen, T. General theory of aerodynamic instability and the mechanism of flutter. *NACA Report No.496* (1979) 291–311.

[11] Zhao, Y. *Aeroelastics and Control*. Science Press, Beijing, 2007. [Chinease]

[12] Zhai1, G., Yoshida, M., Imae1, J. and Kobayash, T. Decentralized H2 Controller Design for Descriptor Systems: An LMI Approach. *Nonlinear Dynamics and Systems Theory* **6**(1) (2006) 99–109.

[13] Gu, Z., Ma, K. and Chen W. *Vibration Active Control*. National Defence Industry Press, Beijing, 1997. [Chinease]